

A MEASUREMENT OF THE ROTATIONAL SPECTRUM OF THE CH RADICAL IN THE FAR-INFRARED^{1,2}

STEVEN A. DAVIDSON³ AND KENNETH M. EVENSON

Time and Frequency Laboratory, National Institute for Standards and Technology, 325 Broadway, Boulder, CO 80303

AND

JOHN M. BROWN

Physical and Theoretical Chemistry Laboratory, South Parks Road, Oxford OX1 3QZ, England

Received 2000 May 16; accepted 2000 June 13

ABSTRACT

Rotational and fine-structure transitions between the lower rotational levels of the CH radical in its X²Π state have been observed in absorption in the laboratory with a tunable far-infrared (TuFIR) spectrometer. The molecules were generated in an electric discharge through a mixture of methane and carbon monoxide in helium. The experimental line widths were limited by Doppler broadening and the measurements have a 1 σ experimental uncertainty of 100 kHz. The frequencies have been used together with all previous measurements of CH in the $v = 0$ level of the X²Π electronic state to determine its molecular parameters and to predict an accurate set of rotational transition frequencies.

Subject headings: ISM: lines and bands — ISM: molecules — methods: laboratory — molecular data

1. INTRODUCTION

It has long been known from the observation of lines in its optical spectrum that the CH radical is an important constituent both of stellar atmospheres (Herzberg 1950) and of the interstellar gas clouds (Dunham & Adams 1937). Indeed, it was one of the first molecules to be identified in the interstellar medium. Only a single line, R₂(1), was observed in the A²Δ–X²Π electronic transition, which was correctly interpreted as an indication of the very low temperature in these gas clouds (Swings & Rosenfeld 1937; McKellar 1940). More recently, its presence in the interstellar medium has been dramatically confirmed by radio astronomy through the detection of lambda-type doubling transitions in the lowest rotational level ($J = \frac{1}{2}$) of the ground ²Π state around 3.3 GHz (Rydbeck, Elldér, & Irvine 1973; Turner & Zuckerman 1974). The corresponding transitions in the next higher rotational level ($J = 1\frac{1}{2}$, F_1) near 710 MHz have also been detected (Ziurys & Turner 1985).

The extent of excitation of CH in different astrophysical sources can be assessed by the observation of spectroscopic transitions that involve higher rotational levels. Such observations can be made through the lambda-doubling transitions in the microwave region or, as has been demonstrated for OH, through rotational transitions in the far-infrared (Storey, Watson, & Townes 1981; Watson et al. 1985). For this reason, considerable effort has been expended in the laboratory to measure the rotational spectrum of the CH radical as accurately as possible. The early experiments involved the use of laser magnetic resonance, in which a molecular transition is tuned into coincidence with a fixed-frequency laser by application of a variable magnetic field (Evenson, Radford, & Moran 1971; Hougen et al.

1978; Brown & Evenson 1983a). Brown & Evenson (1983b) used these measurements to predict the zero-field rotational spectrum of CH with an estimated accuracy of 2.0 MHz. About this time, a new method of recording far-infrared (FIR) spectra was developed in which radiation from two frequency-measured CO₂ lasers, stabilized with saturated fluorescence, was mixed in a fast diode to generate the appropriate FIR difference frequency, the so-called TuFIR method (Evenson, Jennings, & Petersen 1984). In this arrangement, the radiation frequency is tunable over a small range of a few hundred MHz, thereby enabling much more accurate measurements to be made (with an achievable 1 σ uncertainty of 10 kHz). However, the experiment is much less sensitive than laser magnetic resonance because the radiation power levels are very low (a few hundred nanowatts at best).

After OH had been measured by the TuFIR technique (Brown et al. 1986), CH was the next objective for study. We made several measurements on this molecule in 1986 (Davidson 1987) but did not publish them since we could not observe transitions between the two lowest rotational levels around 535 GHz with a great enough signal-to-noise ratio (S/N) to measure them. These transitions are in some ways the most significant of all because they emanate, in absorption, from the lowest rotational level. Despite intermittent attempts to record these transitions, we still have not achieved our objective. Very recently, Amano (2000) has succeeded in observing these transitions with a good S/N in the laboratory using a submillimeter-wave spectrometer with a backward-wave oscillator as radiation source. Accordingly, there is no reason to delay the publication of our results, which cover a wider range of J values, any longer. We have now incorporated Amano's measurements in a fit of all available spectroscopic data on CH in its ground state. With this, we have generated an improved set of molecular parameters that can be used to calculate the most accurate rotational spectrum of CH to date.

2. EXPERIMENTAL DETAILS

The CH transition frequencies were measured with a TuFIR spectrometer in the Boulder laboratories of the

¹We wish to dedicate this paper to our good friend and colleague, Harry Radford, who died on 2000 May 5. His name will live on in association with many groundbreaking pieces of work on the spectroscopy of small molecules, not least with the first detection of the far-infrared spectrum of the CH radical in 1970 March.

²Work supported in part by NASA contract W15, 047.

³Present address: MIT Lincoln Laboratory, 244 Wood Street, Lexington MA 02420.

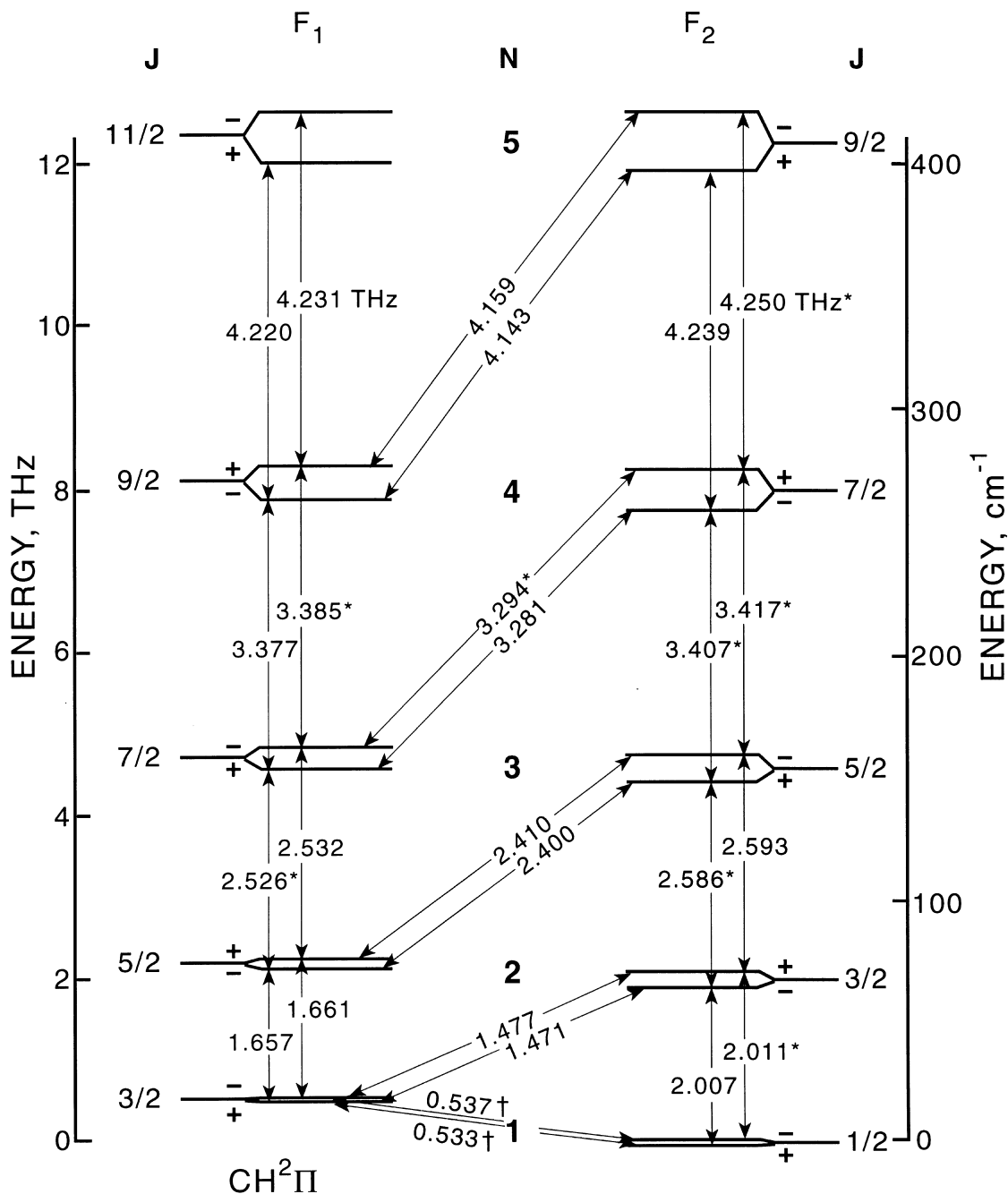


FIG. 1.—Low-lying spin-rotational energy levels of the CH radical, connected by electric dipole transitions (+, \leftrightarrow , -) in the FIR region. The rotational levels conform closely to Hund's case *b* coupling and so are better labeled by the quantum number *N* rather than *J*. The parity (λ -type) doubling has been exaggerated by a factor of 20 for the sake of clarity. The transition frequencies are given in THz. The transitions that have been observed by TuFIR in this work are marked with asterisks. The two transitions observed by Amano (2000) are marked by daggers.

National Institute of Standards and Technology (NIST) in 1986. The system used at that time has been described in some detail elsewhere (Evenson et al. 1984; Nolt et al. 1987) and we give only the essential aspects here. The spectrometer could be operated in either of two modes, second order or third order. In the second-order mixing experiment, radiation from two CO₂ lasers (one of fixed frequency and the other swept by frequency-offset locking to a third laser) was mixed in a nonlinear diode to produce FIR radiation at their difference frequency. In the third-order mode, radiation from two fixed-frequency CO₂ lasers and from a tunable microwave source was mixed in the diode. The mixer was a metal-insulator-metal (MIM) diode. The diode

junction was formed by bringing a tungsten whisker into contact with a metal base; the base was made from nickel for second-order generation and from cobalt for third-order generation. The FIR radiation was emitted from the tungsten wire acting as a long wire antenna. More power was generated in the second-order process (typically 100 nW) but the frequency could only be tuned over the pressure-broadened gain curve of the waveguide CO₂ laser (about ± 120 MHz). The power output in the third-order mode was only a few nanowatts, but the radiation frequency could be tuned over several GHz.

In both modes of operation, the FIR radiation from the diode was collimated with a parabolic reflector, passed

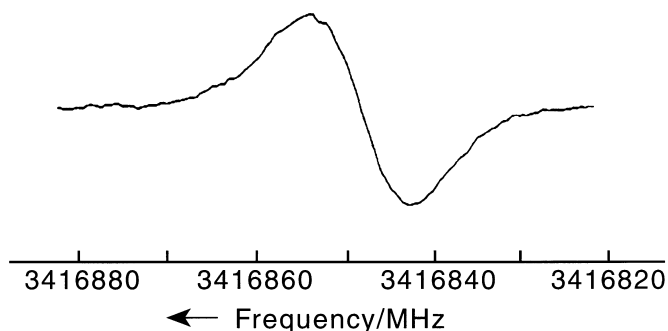


FIG. 2.—An experimental recording of the $J = 3\frac{1}{2}^+ \leftarrow 2\frac{1}{2}^-$, $F_2 \leftarrow F_2$ transition of CH in the $v = 0$ level of the $X^2\Pi$ state (the superscripts indicate the parities of the levels involved). The FIR radiation is frequency modulated; the signal is detected at the modulation frequency so that it appears as the first derivative of an absorption line shape. The signal shown represents the sum of eight back-and-forth scans, each recorded with a 100 ms output time constant. The observed line consists of two proton hyperfine components (with a separation of 4.0 MHz) that are not resolved at Doppler-limited resolution.

through the sample in a 1.5 m long absorption cell, and detected at the other end by a Ge:Ga photoconductor cooled with liquid helium. This detector had an enhanced sensitivity for radiation between 2.5 and 6.0 THz. The FIR radiation was frequency modulated at 1 kHz and the signal detected at this frequency with a lock-in amplifier. Provision was made to scan back and forth through an absorption line and so enhance the S/N by signal averaging. The experimental uncertainty in the frequency measurement, typically 100 kHz, was limited by the precision with which an experimental line center could be identified. The spectrometer accuracy is 10 kHz (Varberg & Evenson 1992).

The CH radical was made in the positive column of a dc electric discharge operating at room temperature. The 1.5 m absorption cell was filled with argon at a pressure between

65 and 133 Pa (between 0.5 and 1.0 torr) together with 0.13 Pa each of carbon monoxide and methane. The discharge current was typically 100 mA. Under these conditions, the experimental line width was set by Doppler broadening. An attempt was made to measure the weak 535 GHz lines of CH by cooling the cell with liquid nitrogen in the hope that this would increase the population of the lower rotational levels. Although the cooling resulted in some changes in the chemistry, it did not increase the strength of transitions between other low-lying levels significantly. The Doppler line widths of these lines indicated a translational temperature of at least 250 K within the discharge. Our method of CH production differs slightly from that of Amano (2000), who used a discharge through a trace of methane in helium to generate the molecule. Amano also reports that the discharge mixtures used by Bogey, Demuynck, & Destombes (1983) did not produce observable amounts of CH in his experiments. It could be that his method produces CH preferentially in lower J levels.

3. RESULTS AND ANALYSIS

Nine rotational transitions of ^{12}CH in the $v = 0$ level of its ground $X^2\Pi$ state were observed in the TuFIR experiment. The observed transitions are marked with asterisks in the spin-rotational energy level of CH shown in Figure 1. The frequencies of six of the transitions were measured using the second-order mixing arrangement and those of the remaining three transitions in the third-order arrangement. The results of these measurements are shown in Table 1. A typical experimental recording is shown in Figure 2; the transition in this case is $J = 3\frac{1}{2}^+ - 2\frac{1}{2}^-$, $F_2 - F_2$. It can be seen that the line width is too broad to allow the proton hyperfine structure to be resolved. Altogether, the hyperfine doublet structure could not be resolved in seven of the lines in Table 1. However, the relative intensities and separations of the hyperfine components can be predicted reliably from

TABLE 1
RAW FREQUENCIES MEASURED IN THE ROTATIONAL SPECTRUM OF THE CH RADICAL IN THE $v = 0$ LEVEL OF ITS GROUND ELECTRONIC STATE

F_i	J	F^a	Measured Frequency (MHz) ^b	Waveguide ^c	Laser I ^d	Isotope in I
$F_1 - F_1$	$3\frac{1}{2} - 2\frac{1}{2}$	$(3^+ - 2^-)$ $(4^+ - 3^-)$	2 525 525.1 ^e	10R (12)	10P (32)	(636) ^f
$F_1 - F_1$	$4\frac{1}{2} - 3\frac{1}{2}$	$(4^+ - 3^-)$ $(5^+ - 4^-)$	3 385 460.7	10R (12)	9R (28)	(626)
$F_2 - F_2$	$1\frac{1}{2} - \frac{1}{2}$	$(1^+ - 0^-)$ $(2^+ - 1^-)$	2 010 811.5	10R (10)	10P (14)	(636)
$F_2 - F_2$	$2\frac{1}{2} - 1\frac{1}{2}$	$(2^+ - 1^-)$ $(3^+ - 2^-)$	2 585 883.0 ^e	10P (18)	9R (20)	(636)
$F_2 - F_2$	$3\frac{1}{2} - 2\frac{1}{2}$	$(3^- - 2^+)$ $(4^- - 3^+)$	3 407 185.1	10R (30)	10P (50)	(636)
$F_2 - F_2$	$3\frac{1}{2} - 2\frac{1}{2}$	$(3^+ - 2^-)$ $(4^+ - 3^-)$	3 416 848.4	9P (26)	10R (18)	(636)
$F_2 - F_2$	$3\frac{1}{2} - 2\frac{1}{2}$	$3^+ - 3^-$	3 416 786.6	9P (26)	10R (18)	(636)
$F_2 - F_2$	$4\frac{1}{2} - 3\frac{1}{2}$	$(4^- - 3^+)$ $(5^- - 4^+)$	4 250 351.6 ^e	9P (32)	10P (24)	(636)
$F_2 - F_1$	$3\frac{1}{2} - 3\frac{1}{2}$	$4^+ - 4^-$	3 294 496.3	9P (22)	10P (30)	(636)

^a Superscripts indicate the parities of the upper and lower hyperfine levels involved.

^b Estimated experimental uncertainty is 100 kHz.

^c Line in tunable CO_2 laser.

^d Line in stabilized CO_2 laser.

^e Frequency measured with third-order FIR generation.

^f CO_2 isotopomer used in stabilized CO_2 laser: (626) corresponds to $^{16}\text{O}^{12}\text{C}^{16}\text{O}$ and (636) corresponds to $^{16}\text{O}^{13}\text{C}^{16}\text{O}$.

TABLE 2
EXPERIMENTAL VALUES FOR TRANSITION FREQUENCIES OF THE CH RADICAL IN ITS GROUND STATE

F_i	J	F	$\nu_{\text{exp}}/\text{MHz}$	OBSERVED-CALCULATED/kHz	REFERENCE
Lambda-type Doubling Frequencies					
F_1	$1\frac{1}{2}$	$1^- \leftarrow 1^{+a}$	724.789 (7) ^b	5	1
		$2^- \leftarrow 2^+$	701.677 (7)	-11	1
F_1	$2\frac{1}{2}$	$2^+ \leftarrow 2^-$	4 847.84 (10)	70	2
		$3^+ \leftarrow 3^-$	4 870.12 (10)	67	2
F_1	$3\frac{1}{2}$	$3^- \leftarrow 4^+$	11 301.22 (20)	-21	2
		$3^- \leftarrow 3^+$	11 287.05 (15)	83	2
		$4^- \leftarrow 4^+$	11 265.21 (15)	219	2
		$4^- \leftarrow 3^+$	11 250.79 (50)	73	2
F_1	$6\frac{1}{2}$	$6^+ \leftarrow 6^-$	43 872.591 (30)	2	3
		$7^+ \leftarrow 7^-$	43 851.026 (30)	-29	3
F_1	$7\frac{1}{2}$	$7^- \leftarrow 7^+$	59 008.076 (20)	24	3
		$8^- \leftarrow 8^+$	59 986.633 (20)	-15	3
F_1	$8\frac{1}{2}$	$8^+ \leftarrow 8^-$	76 168.632 (50)	19	3
		$9^+ \leftarrow 9^-$	76 147.336 (30)	-11	3
F_2	$\frac{1}{2}$	$0^- \leftarrow 1^+$	3 263.794 (3)	0	4
		$1^- \leftarrow 1^+$	3 335.481 (3)	-1	4
		$1^- \leftarrow 0^+$	3 349.193 (3)	0	4
F_2	$1\frac{1}{2}$	$1^+ \leftarrow 2^-$	7 274.78 (15)	-543	5
		$1^+ \leftarrow 1^-$	7 325.15 (15)	-50	5
		$2^+ \leftarrow 2^-$	7 348.28 (15)	-145	5
		$2^+ \leftarrow 1^-$	7 398.38 (15)	78	5
		$2^- \leftarrow 3^+$	14 713.78 (15)	-99	2
F_2	$2\frac{1}{2}$	$2^- \leftarrow 2^+$	14 756.81 (15)	142	2
		$3^- \leftarrow 3^+$	14 778.97 (20)	-11	2
		$3^- \leftarrow 2^+$	14 821.88 (15)	110	2
		$3^+ \leftarrow 4^-$	24 381.57 (40)	90	2
		$3^+ \leftarrow 3^-$	24 420.65 (10)	20	2
F_2	$3\frac{1}{2}$	$4^+ \leftarrow 4^-$	24 442.56 (10)	-27	2
		$4^+ \leftarrow 3^-$	24 482.10 (20)	362	2
		$5^+ \leftarrow 5^-$	50 299.750 (20)	24	3
		$6^+ \leftarrow 6^-$	50 321.276 (20)	-22	3
F_2	$6\frac{1}{2}$	$6^- \leftarrow 6^+$	66 400.098 (30)	22	3
		$7^- \leftarrow 7^+$	66 421.466 (30)	-25	3
Rotational Transition Frequencies					
$F_1 \leftarrow F_1$	$3\frac{1}{2} \leftarrow 2\frac{1}{2}$	$3^+ \leftarrow 2^-$	2 525 528.00 (10) ^b	-184	6
		$4^+ \leftarrow 3^-$	2 525 522.95 (10)	-186	6
$F_1 \leftarrow F_1$	$4\frac{1}{2} \leftarrow 3\frac{1}{2}$	$4^+ \leftarrow 3^-$	3 385 462.20 (10)	88	6
		$5^+ \leftarrow 4^-$	3 385 459.51 (10)	92	6
$F_2 \leftarrow F_2$	$1\frac{1}{2} \leftarrow \frac{1}{2}$	$1^+ \leftarrow 0^-$	2 010 810.46 (10)	-68	6
		$2^+ \leftarrow 1^-$	2 010 811.92 (10)	21	6
$F_2 \leftarrow F_2$	$2\frac{1}{2} \leftarrow 1\frac{1}{2}$	$2^+ \leftarrow 1^-$	2 585 887.32 (10)	232	6
		$3^+ \leftarrow 2^-$	2 585 880.22 (10)	219	6
$F_2 \leftarrow F_2$	$3\frac{1}{2} \leftarrow 2\frac{1}{2}$	$3^- \leftarrow 2^+$	3 407 187.19 (10)	36	6
		$4^- \leftarrow 3^+$	3 407 183.55 (10)	35	6
		$3^+ \leftarrow 2^-$	3 416 850.70 (10)	-416	6
		$4^+ \leftarrow 3^-$	3 416 846.70 (10)	-422	6
		$3^+ \leftarrow 3^-$	3 416 786.59 (10)	576	6
$F_2 \leftarrow F_2$	$4\frac{1}{2} \leftarrow 3\frac{1}{2}$	$4^- \leftarrow 3^+$	4 250 352.95 (10)	4	6
		$5^- \leftarrow 4^+$	4 250 350.53 (10)	2	6
Fine-Structure Transition Frequencies					
$F_2 \leftarrow F_1$	$3\frac{1}{2} \leftarrow 3\frac{1}{2}$	$4^+ \leftarrow 4^-$	3 294 496.33 (10)	-26	6
$F_1 \leftarrow F_2$	$1\frac{1}{2} \leftarrow \frac{1}{2}$	$1^+ \leftarrow 1^-$	532 721.333 (100)	-331	7
		$2^+ \leftarrow 1^-$	532 723.926 (40)	-42	7
		$1^+ \leftarrow 0^-$	532 793.309 (50)	-44	7
		$2^- \leftarrow 1^+$	536 761.145 (50)	17	7
		$1^- \leftarrow 1^+$	536 781.945 (50)	23	7
		$1^- \leftarrow 0^+$	536 795.678 (50)	37	7

^a Superscripts indicate the parities of the upper and lower levels involved.

^b Estimated experimental uncertainty, in units of the last quoted decimal place.

REFERENCES.—(1) Ziurys & Turner 1985; (2) Brazier & Brown 1983; (3) Bogey et al. 1983; (4) Rydbeck et al. 1974; (5) Brazier & Brown 1984; (6) this work; (7) Amano 2000.

TABLE 3
MOLECULAR PARAMETERS FOR THE CH RADICAL IN
THE $v = 0$ LEVEL OF THE $X^2\Pi$ STATE^a

Parameter	Present Work	Previous Value ^b
A_0	834 818.508 (55) ^c	843 817.57 (69)
A_D	0.0 ^d	0.0 ^d
B_0	425 476.222 (45)	425 476.852 (73)
D_0	43.7857 (28)	43.8255 (32)
$10^2 H_0$	0.3173 (55)	0.350 ^d
γ	-772.106 (25)	-771.11 (26)
γ_D	0.2584 (27)	0.158 (24)
p	1003.9958 (57)	1003.9957 (23)
p_D	-0.27366 (66)	-0.27335 (28)
$10^4 p_H$	0.34 (12)	0.326 (49)
q	1159.6832 (28)	1159.6830 (12)
q_D	-0.45749 (11)	-0.457479 (47)
$10^4 q_H$	0.964 (12)	0.9632 (51)
a	54.006 (80)	54.28 (14)
b_F	-57.777 (68)	-57.67 (20)
c	56.52 (25)	57.17 (17)
d	43.513 (11)	43.5167 (40)
$10 d_D$	-0.157 (12)	-0.1601 (52)
$10^2 C'_1$	0.0 ^d	0.56 (17)

^a Values in MHz.

^b Values determined by Brazier & Brown 1984.

^c Figures in parentheses represent one standard deviation of the least-squares fit, in units of the last quoted decimal place.

^d Parameter constrained to this value in the least-squares fits.

earlier measurements made by microwave-optical double resonance (Brazier & Brown 1983, 1984). Before fitting the transition frequencies of CH to obtain molecular parameters, each of the unresolved rotational transitions was deconvolved into its associated hyperfine doublet on the assumption that the measured line center occurred at the intensity-weighted mean of the two components. The individual hyperfine transition frequencies obtained in this way are given in Table 2.

Table 2 lists all the available experimental measurements of the lambda-doubling, rotational, and spin-rotational transition frequencies of ^{12}CH in the $v = 0$ level of its $X^2\Pi$ state. These are drawn from astrophysical observations (Rydbeck et al. 1974; Ziurys & Turner 1985), microwave-optical double resonance (Brazier & Brown 1983, 1984), microwave spectroscopy (Bogey, Demuynck, & Destombes 1983), submillimeter-wave spectroscopy (Amano 2000), and the present work. This data set has been used to determine the parameters of an effective Hamiltonian for a diatomic molecule in an isolated electronic state. The details of this Hamiltonian are given elsewhere (e.g., Brown & Evenson 1983a). Each datum was weighted as the inverse of the square of its experimental uncertainty in the fit. The parameter A_D cannot be determined separately from the spin-rotation parameter γ (Brown & Watson 1977) and so was constrained to zero in the fit. The results are given in Table 2 (residuals) and Table 3 (parameter values). The standard deviation of the fit relative to the estimated experimental error was 1.90; we believe that this figure reflects slightly overoptimistic estimates of experimental uncertainties in some cases (see Table 2). For this reason, we have chosen not to include the small hyperfine parameter C'_1 in our model, even though it was determined by Brazier & Brown

(1984). Its inclusion improves the quality of our fit slightly, but we do not think that its value is meaningful.

4. DISCUSSION

The parameters derived in the present work are compared with those obtained previously by Brazier & Brown (1984) in Table 3. Because the data set now contains more accurate measurements of spin and rotational intervals, the major parameters representing spin-orbit coupling (A_0), rotational kinetic energy (B_0), and spin-rotation coupling (γ_0) are significantly better determined. Furthermore, we are now able to determine the sextic centrifugal distortion parameter (H_0), whereas in the previous fit, it was constrained to a value estimated from theory.

Brown & Evenson (1983b) published a calculated rotational spectrum of CH based on observations made by FIR laser magnetic resonance, a more sensitive but less accurate method of recording spectroscopic transitions in this wavelength region. There is a need to update this table, not just because of the availability of better data but because the analysis of the laser magnetic resonance spectrum by Brown and Evenson contained a misassignment that degrades its reliability (Brazier & Brown 1984). The computed values of the transition frequencies of individual hyperfine transitions involving all rotational levels up to $N = 5$ are given in Table 4. We have also included the standard error (1σ) for each frequency, estimated from the variance-covariance matrix of the parameters determined in the fit. The uncertainties range from 36 kHz (for the 536.8 GHz transition) to 292 kHz (for the 4219.8 GHz transition). The important spin-rotational transitions of CH have also been summarized in the energy level diagram of Figure 1. The computed transition line strengths $S_{F,F'}$, which are also listed in Table 4, can be used to assess the relative intensities of individual transitions. The line strength is defined by

$$S_{F,F'} = | \langle \gamma' F' || \mathcal{D}_q^{(1)}(\omega) * || \gamma F \rangle |^2, \quad (1)$$

where the quantity on the right-hand side is the reduced matrix element of the rotation matrix (Brink & Satchler 1993) and γ stands for subsidiary quantum numbers. The intensity of a line in absorption can be obtained by multiplying the line strength by the square of the dipole moment μ (1.46 D for CH, Phelps & Dalby 1966), by the transition frequency, and by the population difference between the lower and upper states. The Einstein A -coefficients for spontaneous emission from state i to j can also be calculated from the line strengths by use of

$$A_{i \rightarrow j} = (16\pi^3 \nu_{ij} / 3\epsilon_0 hc^3) (2F_i + 1)^{-1} S_{ij} \mu^2. \quad (2)$$

Table 4 is not quite complete because the transitions with $\Delta J = 1$, $F_2 \leftarrow F_1$ have been omitted. Although these transitions are formally allowed, they are very weak because they also require $\Delta N = 2$ and so would be forbidden in the Hund's case b limit (to which CH conforms closely in its ground $^2\Pi$ state).

Although the present paper combined with that of Amano (2000) represents a significant step forward in our knowledge of the energy levels of CH, there is still room for improvement. Many of the microwave lambda-doubling intervals could be measured more accurately (see Table 2), and it is desirable to measure more of the FIR spin-rotational transition frequencies. The recent availability of

TABLE 4
CALCULATED SPIN-ROTATION TRANSITION FREQUENCIES FOR THE CH RADICAL IN ITS GROUND STATE

TRANSITION ^a			FREQUENCY (GHz)	VACUUM WAVELENGTH (μm)	LINE STRENGTH ^b
$F'_i-F''_i$	$J'-J''$	$F'-F''$			
A. $\Delta N = 1, \Delta J = 1$ Transitions					
F_1-F_1	$2\frac{1}{2}-1\frac{1}{2}$	$3^- - 2^+$	1656.96117 (13) ^c	180.92908	2.3070
		$2^- - 2^+$	1656.97039 (15)	180.92807	0.1647
		$2^- - 1^+$	1656.97270 (14)	180.92782	1.4831
		$3^+ - 2^-$	1661.10726 (13)	180.47748	2.3090
		$2^+ - 1^-$	1661.11797 (13)	180.47632	1.4844
		$2^+ - 2^-$	1661.13876 (13)	180.47406	0.1649
F_1-F_1	$3\frac{1}{2}-2\frac{1}{2}$	$4^+ - 3^-$	2525.52314 (9) ^d	118.70509	3.5271
		$3^+ - 2^-$	2525.52818 (9) ^d	118.70485	2.6127
		$3^+ - 3^-$	2525.53741 (11)	118.70442	0.1306
		$4^- - 3^+$	2531.94036 (9)	118.40423	3.5284
		$3^- - 2^+$	2531.94510 (9)	118.40401	2.6137
		$3^- - 3^+$	2531.97661 (11)	118.40254	0.1306
F_1-F_1	$4\frac{1}{2}-3\frac{1}{2}$	$5^- - 4^+$	3376.79122 (13)	88.78028	4.6404
		$4^- - 3^+$	3376.79409 (13)	88.78020	3.6913
		$4^- - 4^+$	3376.80836 (14)	88.77983	0.1054
		$5^+ - 4^-$	3385.45942 (13) ^d	88.55296	4.6414
		$4^+ - 3^-$	3385.46211 (13) ^d	88.55289	3.6920
		$4^+ - 4^-$	3385.49836 (14)	88.55194	0.1054
F_1-F_1	$5\frac{1}{2}-4\frac{1}{2}$	$6^+ - 5^-$	4219.78636 (29)	71.04446	5.7099
		$5^+ - 4^-$	4219.78823 (29)	71.04443	4.7437
		$5^+ - 5^-$	4219.80538 (29)	71.04414	0.8777×10^{-1}
		$6^- - 5^+$	4230.66566 (29)	70.86177	5.7107
		$5^- - 4^+$	4230.66740 (29)	70.86174	4.7443
		$5^- - 5^+$	4230.70634 (29)	70.86109	0.8781×10^{-1}
F_2-F_2	$1\frac{1}{2}-\frac{1}{2}$	$1^- - 1^+$	2006.74912 (14)	149.39210	0.1671
		$1^- - 0^+$	2006.76283 (14)	149.39108	0.3342
		$2^- - 1^+$	2006.79900 (12)	149.38838	0.8355
		$1^+ - 1^-$	2010.73884 (14)	149.09567	0.1679
		$1^+ - 0^-$	2010.81053 (14) ^d	149.09036	0.3357
		$2^+ - 1^-$	2010.81194 (12) ^d	149.09025	0.8392
F_2-F_2	$2\frac{1}{2}-1\frac{1}{2}$	$2^+ - 2^-$	2585.83721 (13)	115.93632	0.1651
		$3^+ - 2^-$	2585.88000 (9) ^d	115.93440	2.3105
		$2^+ - 1^-$	2585.88709 (9) ^d	115.93409	1.4853
		$2^- - 2^+$	2593.24545 (13)	115.60512	0.1652
		$3^- - 2^+$	2593.31056 (9)	115.60222	2.3125
		$2^- - 1^+$	2593.31856 (9)	115.60186	1.4866
F_2-F_2	$3\frac{1}{2}-2\frac{1}{2}$	$3^- - 3^+$	3407.14436 (11)	87.989362	0.1307
		$4^- - 3^+$	3407.18352 (7) ^d	87.988350	3.5284
		$3^- - 2^+$	3407.18715 (7) ^d	87.988256	2.6136
		$3^+ - 3^-$	3416.78601 (11) ^d	87.741070	0.1308
		$4^+ - 3^-$	3416.84712 (7) ^d	87.739500	3.5297
		$3^+ - 2^-$	3416.85112 (7) ^d	87.739397	2.6146
F_2-F_2	$4\frac{1}{2}-3\frac{1}{2}$	$4^+ - 4^-$	4238.44893 (16)	70.731643	0.1055
		$5^+ - 4^-$	4238.48588 (13)	70.731027	4.6410
		$4^+ - 3^-$	4238.48808 (13)	70.730990	3.6917
		$4^- - 4^+$	4250.29184 (16)	70.534559	0.1055
		$5^- - 4^+$	4250.35053 (13) ^d	70.533584	4.6420
		$4^- - 3^+$	4250.35295 (13) ^d	70.533544	3.6925

TABLE 4—Continued

TRANSITION ^a			FREQUENCY (GHz)	VACUUM WAVELENGTH (μm)	LINE STRENGTH ^b		
$F'_i-F''_i$	$J'-J''$	$F'-F''$					
B. $\Delta N = 1, \Delta J = 0$ Transitions							
F_2-F_1	$1\frac{1}{2}-1\frac{1}{2}$	$1^- - 2^+$	1470.68967 (14)	203.84481	0.3363×10^{-1}		
		$1^- - 1^+$	1470.69197 (14)	203.84449	0.1681		
		$2^- - 2^+$	1470.73955 (12)	203.83790	0.3028		
		$2^- - 1^+$	1470.74185 (13)	203.83758	0.3359×10^{-1}		
		$1^+ - 1^-$	1477.29239 (14)	202.93373	0.1652		
	F_2-F_1	$2\frac{1}{2}-2\frac{1}{2}$	$1^+ - 2^-$	1477.31319 (14)	202.93088	0.3303×10^{-1}	
			$2^+ - 1^-$	1477.36549 (13)	202.92369	0.3301×10^{-1}	
			$2^+ - 2^-$	1477.38630 (12)	202.92083	0.2974	
			$2^+ - 2^-$	2399.60637 (16)	124.93402	0.1344	
			$2^+ - 3^-$	2399.61559 (14)	124.93353	0.9603×10^{-2}	
F_2-F_1		$3\frac{1}{2}-3\frac{1}{2}$	$3^+ - 2^-$	2399.64915 (13)	124.93179	0.9577×10^{-2}	
			$3^+ - 3^-$	2399.65838 (14)	124.93131	0.1921	
			$2^- - 2^+$	2409.49298 (16)	124.42139	0.1322	
			$2^- - 3^+$	2409.52449 (14)	124.41976	0.9446×10^{-2}	
			$3^- - 2^+$	2409.55808 (13)	124.41862	0.9429×10^{-2}	
	F_2-F_1	$4\frac{1}{2}-4\frac{1}{2}$	$3^- - 3^+$	2409.58959 (13)	124.41640	0.1890	
			$3^- - 3^+$	3281.26534 (19)	91.364895	0.1079	
			$3^- - 4^+$	3281.27961 (18)	91.364496	0.4001×10^{-2}	
			$4^- - 3^+$	3281.30449 (16)	91.363803	0.3981×10^{-2}	
			$4^- - 4^+$	3281.31876 (17)	91.363406	0.1401	
F_2-F_1		$4\frac{1}{2}-4\frac{1}{2}$	$3^+ - 3^-$	3294.39900 (19)	91.000652	0.1063	
			$3^+ - 4^-$	3294.43525 (17)	90.999651	0.3937×10^{-2}	
			$4^+ - 3^-$	3294.46011 (17)	90.998964	0.3924×10^{-2}	
			$4^+ - 4^-$	3294.49636 (17) ^d	90.997963	0.1378	
			$4^+ - 4^-$	4142.95933 (26)	72.361911	0.8953×10^{-1}	
	F_2-F_1	$4\frac{1}{2}-4\frac{1}{2}$	$4^+ - 5^-$	4142.97647 (25)	72.361611	0.2037×10^{-2}	
			$5^+ - 4^-$	4142.99628 (25)	72.361267	0.2021×10^{-2}	
			$5^+ - 5^-$	4143.01342 (25)	72.360967	0.1100	
			$4^- - 4^+$	4159.28983 (26)	72.077800	0.8815×10^{-1}	
			$4^- - 5^+$	4159.32878 (25)	72.077125	0.2004×10^{-2}	
$5^- - 5^+$		$5^- - 4^+$	4159.34852 (25)	72.076783	0.1993×10^{-2}		
		$5^- - 5^+$	4159.38747 (25)	72.076107	0.1083		
		C. $\Delta N = 0, \Delta J = 1$ Transitions					
		F_1-F_2	$1\frac{1}{2}-\frac{1}{2}$	$1^+ - 1^-$	532.72166 (4) ^d	562.75627	0.1655
				$2^+ - 1^-$	532.72397 (4) ^d	562.75384	0.8274
$1^+ - 0^-$	532.79335 (4) ^d			562.68055	0.3309		
$2^- - 1^+$	536.76113 (4) ^d			558.52118	0.8312		
$1^- - 1^+$	536.78193 (4) ^d			558.49953	0.1662		
$1^- - 0^+$	536.79564 (4) ^d			558.48527	0.3324		
F_1-F_2	$2\frac{1}{2}-1\frac{1}{2}$	$3^- - 2^+$	178.87319 (15)	1676.005	0.2415×10^{-1}		
		$2^- - 2^+$	178.88242 (15)	1675.919	0.1732×10^{-2}		
		$2^- - 1^+$	178.95552 (18)	1675.234	0.1551×10^{-1}		
		$3^+ - 2^-$	191.06939 (15)	1569.024	0.2407×10^{-1}		
		$2^+ - 2^-$	191.10090 (15)	1568.765	0.1718×10^{-2}		
		$2^+ - 1^-$	191.15078 (18)	1568.355	0.1546×10^{-1}		
F_1-F_2	$3\frac{1}{2}-2\frac{1}{2}$	$4^+ - 3^-$	111.08577 (16)	2698.748	0.7507×10^{-2}		
		$3^+ - 3^-$	111.10005 (16)	2698.401	0.2813×10^{-3}		
		$3^+ - 2^-$	111.16515 (19)	2696.821	0.5552×10^{-2}		
		$4^- - 3^+$	137.12975 (16)	2186.195	0.7491×10^{-2}		
		$3^- - 3^+$	137.16600 (16)	2185.618	0.2765×10^{-3}		
		$3^- - 2^+$	137.20879 (19)	2184.936	0.5541×10^{-2}		
F_1-F_2	$4\frac{1}{2}-3\frac{1}{2}$	$5^- - 4^+$	71.02987 (21)	4220.653	0.3310×10^{-2}		
		$4^- - 4^+$	71.04701 (21)	4219.634	0.7701×10^{-4}		
		$4^- - 3^+$	71.10812 (23)	4216.009	0.2627×10^{-2}		
		$5^+ - 4^-$	115.40565 (21)	2597.727	0.3305×10^{-2}		
		$4^+ - 4^-$	115.44459 (21)	2596.851	0.7449×10^{-4}		
		$4^+ - 3^-$	115.48374 (23)	2595.971	0.2624×10^{-2}		

^a Quantum numbers for the upper and lower states are denoted by single and double primes, respectively. Superscripts on the F quantum number values indicate parities of the states involved in accordance with the definition in Brown et al. 1978.

^b For definition, see eq. (1).

^c Estimated standard error in the calculated frequency, in units of the last quoted decimal place (1 σ).

^d Transition observed in the laboratory.

high-power backward-wave oscillators (Winnewisser 1995; Lewen et al. 1997) suggests that all the lower frequency rotational transitions can now be measured with good sensitivity and accuracy.

We are very grateful to Dr. Filippo Tamassia for help with the computation involved in this work.

REFERENCES

- Amano, T. 2000, ApJ, 531, L161
Bogey, M., Demuyck, C., & Destombes, J. L. 1983, Chem. Phys. Lett., 100, 105
Brazier, C. R., & Brown, J. M. 1983, J. Chem. Phys., 78, 1608
———, 1984, Canadian J. Phys., 62, 1563
Brink, D. M., & Satchler, G. R. 1993, Angular Momentum (3d ed.; Oxford: Oxford Univ. Press)
Brown, J. M., & Evenson, K. M. 1983a, J. Mol. Spectrosc., 98, 392
———, 1983b, ApJ, 268, L51
Brown, J. M., Evenson, K. M., Jennings, D. A., Zink, L. R., Hinz, A., & Nolt, I. G. 1986, ApJ, 307, 410
Brown, J. M., Kaise, M., Kerr, C. M. L., & Milton, D. J. 1978, Mol. Phys., 36, 553
Brown, J. M., & Watson, J. K. G. 1977, J. Mol. Spectrosc., 65, 65
Davidson, S. A. 1987, Ph.D. thesis, Univ. Colorado
Dunham, T., & Adams, W. S. 1937, PASP, 49, 26
Evenson, K. M., Jennings, D. A., & Petersen, F. R. 1984, App. Phys. Lett., 44, 576
Evenson, K. M., Radford, H. E. & Moran, M. M. 1971, App. Phys. Lett., 18, 426
Herzberg, G. 1950, Molecular Spectra and Molecular Structure, Vol. 1, Spectra of Diatomic Molecules (New York: Van Nostrand)
Hougen, J. T., Mucha, J. A., Jennings, D. A., & Evenson, K. M. 1978, J. Mol. Spectrosc., 72, 463
Lewen, F., Michael, E., Gendriesch, R., Stutzki, J. & Winnewisser, G. 1997, J. Mol. Spectrosc., 183, 207
McKellar, A. 1940, PASP, 52, 307
Nolt, I. G., et al. 1987, J. Mol. Spectrosc., 125, 274
Phelps, D. H., & Dalby, F. W. 1966, Phys. Rev. Lett., 16, 3
Rydbeck, O. E. H., Elldér, J., & Irvine, W. M. 1974, Nature, 246, 466
Storey, J. W. V., Watson, D. M., & Townes, C. H. 1981, ApJ, 244, L27
Swings, P., & Rosenfeld, L. 1937, ApJ, 86, 483
Turner, B. E., & Zuckerman, B. 1974, ApJ, 187, L59
Varberg, T. D., & Evenson, K. M. 1992, ApJ, 385, 763
Watson, D. M., Genzel, R., Townes, C. H., & Storey, J. W. V. 1985, ApJ, 298, 316
Winnewisser, G. 1995, Vibr. Spectrosc., 8, 241
Ziurys, L. M., & Turner, B. E. 1985, ApJ, 292, L25